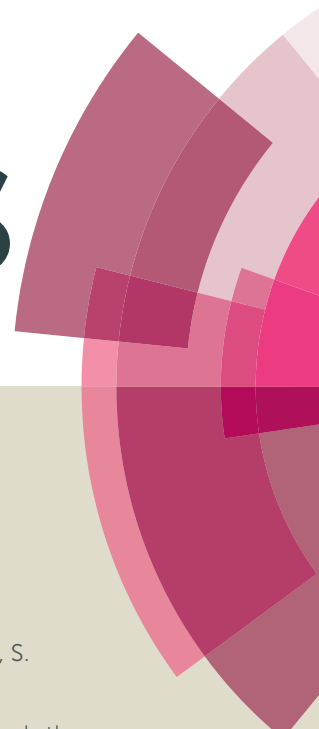


RSC Advances



This article can be cited before page numbers have been issued, to do this please use: J. Ye, B. Cheng, S. Wageh, A. A. Al-Ghamdi and J. Yu, *RSC Adv.*, 2016, DOI: 10.1039/C6RA02569B.



This is an *Accepted Manuscript*, which has been through the Royal Society of Chemistry peer review process and has been accepted for publication.

Accepted Manuscripts are published online shortly after acceptance, before technical editing, formatting and proof reading. Using this free service, authors can make their results available to the community, in citable form, before we publish the edited article. This *Accepted Manuscript* will be replaced by the edited, formatted and paginated article as soon as this is available.

You can find more information about *Accepted Manuscripts* in the [Information for Authors](#).

Please note that technical editing may introduce minor changes to the text and/or graphics, which may alter content. The journal's standard [Terms & Conditions](#) and the [Ethical guidelines](#) still apply. In no event shall the Royal Society of Chemistry be held responsible for any errors or omissions in this *Accepted Manuscript* or any consequences arising from the use of any information it contains.



RSC Adv.

ARTICLE

Flexible Mg-Al Layered Double Hydroxide Supported Pt on the Al foil for use in Room-Temperature catalytic decomposition of formaldehyde

Received 00th January 20xx,
Accepted 00th January 20xx

DOI: 10.1039/x0xx00000x

www.rsc.org/

Jiawei Ye,^a Bei Cheng,^a S. Wageh,^b Ahmed A. Al-Ghamdi^b and Jiaguo Yu^{a,b,*}

Room-temperature catalytic decomposition of formaldehyde (HCHO) is regarded as one of the best methods for indoor HCHO purification and removal. Herein, for the first time, flexible and bendable Mg-Al layered double hydroxide (LDH) on aluminum (Al) foil was in-situ prepared and further decorated by platinum (Pt) nanoparticles (NPs) for catalytic oxidation decomposition of HCHO at room temperature. Such a Pt-loaded large-area flexible LDH catalyst can be directly used and easily regenerated because of its flexibility and relatively low production cost. Moreover, it exhibited an excellent catalytic performance toward oxidation decomposition of HCHO at room temperature due to its hierarchical macro-/mesoporous structure that facilitates the diffusion of reactants and products. Furthermore, abundant hydroxyl groups on the catalyst surface are also beneficial to the HCHO oxidation decomposition. This work may provide some new insight into the design and fabrication of advanced catalyst for indoor HCHO removal and air purification.

1. Introduction

HCHO is recognized as a major indoor air pollutant. Recently, unprecedented use of building and furnishing materials results in a higher emission of indoor HCHO than ever. Prolonged exposure to even a few parts per million (ppm) of HCHO may cause serious health problems including respiratory diseases, nasal tumors and skin irritation.¹⁻³ Therefore, the development of efficient methods and materials for the removal of indoor HCHO is essential to meet human health needs.

Many methods such as adsorption (physical adsorption,⁴⁻¹⁰ chemisorption¹¹⁻¹³), plasma technical oxidation,¹⁴⁻¹⁶ photocatalytic degradation¹⁷⁻¹⁹ and thermal catalytic oxidation decomposition^{2,20-32} have been investigated and developed for the removal of indoor formaldehyde in air. Among these methods, HCHO removal by room temperature catalytic oxidation decomposition offers a feasible strategy for solving this important environmental problem. By using room-temperature catalytic oxidation technology, the toxic formaldehyde can be completely decomposed into carbon dioxide and water. Also, no additional apparatus and energy are needed comparing with conventional high-temperature thermal catalytic oxidation and photocatalytic methods. To date, a lot of oxide-supported noble metal catalysts, such as Pt/TiO₂,^{2,21,24,25,33-35} Pt/Fe₂O₃,³⁶ Pd/TiO₂,^{20,27} Pt/SiO₂,²² Pt/Al₂O₃,²³ Au/CeO₂,²⁹ and Au/Co₃O₄-CeO₂³⁷ have been studied for room-temperature catalytic oxidation decomposition of formaldehyde. However, most of the above mentioned catalysts were mainly fabricated by using powders

composed of NPs as the supports of noble metals. Practically, such catalysts in the form of powders need to be adhered to other big-block substrates, requiring complicated processes and extra cost. Moreover, it is of great difficulties in regenerating and recycling the powder formed catalysts. To overcome the aforementioned drawbacks of powder samples, flexible catalysts based on metal foils will attract wider research interests due to their good flexibility, light weight, and low cost.

Herein, flexible Mg-Al LDH on Al foil (LDH-Foil) was first prepared by in situ growth technique on the Al foil by means of hydrothermal method in the presence of urea and magnesium nitrate. The prepared flexible LDH-Foil sheet was then used as the supporting materials of Pt NPs obtained by NaBH₄ reduction method. Particularly, this flexible and bendable macro-sized Mg-Al LDH-Al foil supported Pt catalyst (Pt-LDH-Foil) with ~20 μm thickness LDH layer exhibited good HCHO oxidation activity, which can be directly used without further modification or remodeling of the catalyst. Thus, it is convenient to recycle the catalyst and to retrieve rare metals in the catalyst after application. Considering the facile preparation procedure of the Pt-LDH-Foil catalyst, this work will provide some new insight into the design and fabrication of new flexible and high-efficiency catalytic materials for indoor formaldehyde decomposition.

2. Experimental section

All chemicals used in this study were reagent-grade without further treatment. Distilled water was used in the whole experiment. Al foils were cleaned in ethanol and deionized water before use.

Preparation of Mg-Al LDH-Foil

The flexible Mg-Al LDH-Foil was fabricated by in situ growth method onto commercial aluminium foil (with thicknesses of ca. 20

^a State Key Laboratory of Advanced Technology for Materials Synthesis and Processing, Wuhan University of Technology, Luoshi Road 122, Wuhan, 430070, China

^b Department of Physics, Faculty of Science, King Abdulaziz University, Jeddah 21589, Saudi Arabia.

† Footnotes relating to the title and/or authors should appear here.

Electronic Supplementary Information (ESI) available: [details of any supplementary information available should be included here]. See DOI: 10.1039/x0xx00000x

ARTICLE

Journal Name

μm in rectangular shapes with dimensions of $100 \text{ mm} \times 200 \text{ mm}$) using hydrothermal method similar to the previously report by He et al.³⁸ In a typical preparation, 9.7 g urea and 6.9 g $\text{Mg}(\text{NO}_3)_2 \cdot 6\text{H}_2\text{O}$ were dissolved in 500 mL deionized water in a glass vessel. The cleaned Al foil with thickness of about 0.02 mm and a size of $10 \times 20 \text{ cm}^2$ was immersed into the solution and the glass vessel was sealed, maintained at $80 \text{ }^\circ\text{C}$ for 48 h. After hydrothermal reaction, cooling to the room temperature, Mg-Al LDH on the Al foil were washed with deionized water and dried at $80 \text{ }^\circ\text{C}$ for 6 h to obtain the LDH-Foil sample.

Preparation of Pt loaded catalyst

In a typical preparation, a round piece of LDH-Foil (10 cm in diameter) was placed on the bottom of glass Petri dish with a diameter of 10 cm. Then, 10 ml of NaBH_4 ethanol solution (0.05 mol/L) was added into the dish. After impregnation for 10 minutes, the solution was discarded and 2 ml of H_2PtCl_6 ethanol solution (6.10 mmol/L) was added dropwise onto the LDH-Foil. After that, an extra 2 ml of NaBH_4 ethanol solution (0.05 mol/L) was added to the dish. Then, the sample was dried at $80 \text{ }^\circ\text{C}$ for 1 h. Finally, the as-obtained products were washed with deionized water to remove chloride anions and then dried at $80 \text{ }^\circ\text{C}$ for 6 h. The real Pt loading in the Pt-LDH-Foil sample measured by inductively coupled plasma atomic emission spectrometry (ICP-AES) was about 0.223 wt%. For comparison, Pt loaded Al foil (Pt-Al-Foil) was also prepared by the above process.

Characterization

The phase structures of Al foil, LDH-Foil and Pt-LDH-Foil were analysed by a D/Max-RB X-ray diffractometer (Rigaku, Japan) with Cu $K\alpha$ radiation at a scan rate (2θ) of 0.05 s^{-1} . The morphology observation was performed by a JSM-6510 scanning electron microscopy (SEM, JEOL, Japan) at an accelerating voltage of 20 kV. Transmission electron microscopy (TEM) images were collected on a JEM-2100F microscopy at an accelerating voltage of 200 kV. The elemental analysis of Pt-LDH-Foil sample were performed by using Field emission scanning electron microscope (FESEM, JEOL 7500F, Japan) equipped with an energy dispersive X-ray (EDX) system operating at an accelerating voltage of 15 kV. X-ray photoelectron spectra (XPS) measurements were carried out on VG ESCALAB210 with Mg $K\alpha$ source. All binding energies were referenced to the C 1s peak at 285.0 eV of the surface adventitious carbon. The Brunauer-Emmett-Teller (BET) specific surface area (S_{BET}) of the samples (the powder peeled off from the foil) was analysed in a nitrogen adsorption apparatus (Micromeritics ASAP 2020, USA). Prior to nitrogen adsorption measurements, all of the samples were degassed at $180 \text{ }^\circ\text{C}$. The BET surface area was determined by a multipoint method using adsorption data in the relative pressure (P/P_0) range of 0.05–0.3. The pore size distribution curves were obtained via the Barret-Joyner-Halender (BJH) method assuming a cylindrical pore model using the nitrogen adsorption isotherm. The pore volume and the average pore size were calculated using the nitrogen adsorption volume at a relative pressure (P/P_0) of 0.97. In situ diffuse Fourier transform infrared spectroscopy (DFTIRS) was recorded on Thermo Fisher IS50. Before the beginning of the DFTIR experiments, the catalyst was swept by pure

O_2 gas for 60 min. And then, the reactant gas mixture ($\text{HCHO} + \text{O}_2$) was introduced into the DFTIR cell at room temperature via mass flow controllers at a flow rate of 30 mL/min. All spectra were recorded with a resolution of 4 cm^{-1} , and the background spectrum was subtracted from each spectrum, respectively.

Catalytic activity characterization

Room-temperature catalytic oxidation decomposition of HCHO was performed in a dark organic glass box covered by a layer of Al foil paper on its inner wall at $25 \text{ }^\circ\text{C}$. A round piece of catalyst (10 cm in diameter) was placed on the bottom of a glass Petri dish with a diameter of 10 cm. After placing the sample-contained dish into the bottom of reactor with a glass slider, 8 μL of condensed HCHO solution (38 wt%) was injected into the reactor and a 5 W fan was placed in the bottom of reactor during the whole reaction process. After 1 h, the HCHO solution was completely volatilized and the concentration of HCHO got stabilized. The concentrations of HCHO, CO_2 , CO and water vapour were online detected by a Photoacoustic IR Multigas Monitor (INNOVA air Tech Instruments Model 1412). The HCHO vapour was allowed to reach adsorption/desorption equilibrium with the reactor surface before the catalytic test. The beginning concentration of HCHO after equilibrium was controlled at ca. 200 ppm. The catalytic oxidation reaction of HCHO started right after the glass slide cover over the Petri dish was removed. The increase of CO_2 concentration (ΔCO_2) and the decrease of HCHO concentration were used to evaluate the catalytic performance of the prepared samples.

3. Results and discussion

Phase structure and morphology

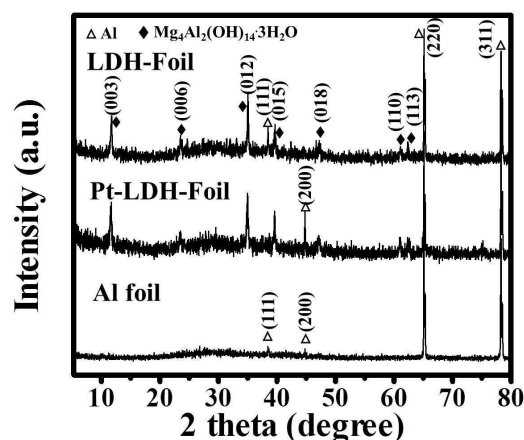


Figure 1. XRD patterns of LDH-Foil, Pt-LDH-Foil and Al foil samples.

X-ray diffraction (XRD) was used to investigate the changes in crystallographic structure of the as-prepared samples before and after hydrothermal treatment and Pt loading. Figure 1 shows the comparison of XRD patterns of LDH-Foil, Pt-LDH-Foil and Al foil samples. The diffraction peaks marked with \blacklozenge and \triangle can be assigned to Mg-Al hydroxide hydrate (JCPDS No. 35-0964) and Al (JCPDS No. 04-0787), respectively. The Al foil before hydrothermal treatment has only metallic Al phase. After hydrothermal treatment,

phase composition of the LDH-Foil sample has a significant change from metallic Al to both Mg-Al hydroxide hydrate and metallic Al. The appearance of the Mg-Al hydroxide hydrate phase is ascribed to the growth of Mg-Al LDH layer on the surface of Al foil. The XRD pattern of the Pt-LDH-Foil sample is similar to that of the LDH-Foil sample, indicating that the Pt loading has no obvious effect on the phase structure of LDH-Foil sample. No any diffraction peaks of Pt are observed in the XRD pattern of Pt-LDH-Foil sample mainly due to Pt with low amount, small particle size and weak crystallization.^{20,25}

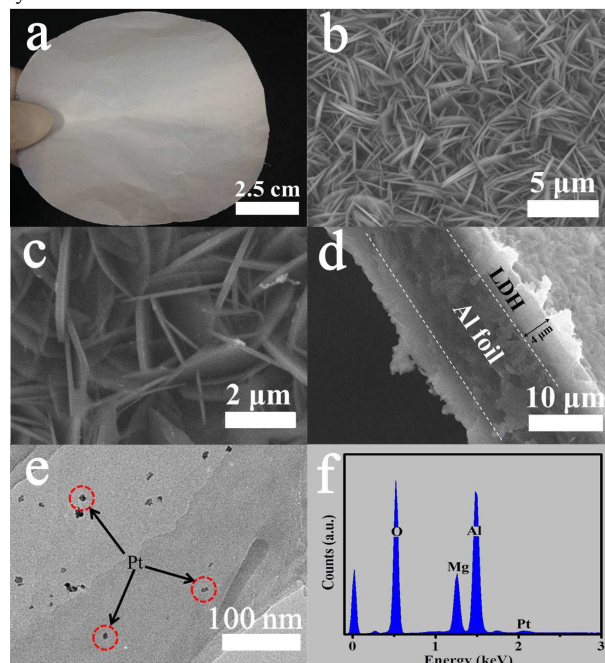


Figure 2. Macroscopic photograph (a) of Pt-LDH-Foil sample, SEM images (b), high magnification SEM image (c), cross-section SEM image (d), TEM image (e) and EDX spectrum (f) of Pt-LDH-Foil sample.

The prepared Pt-LDH-Foil sample exhibits good flexibility and deformability, which can be bent to different shapes without damaging it just as the Al foil can. Figure 2a presents the camera photograph of Pt-LDH-Foil sample, indicating that the surface appears grey and black colour due to the formation of LDH on the Al foil and deposition of Pt NPs. The morphology and surface microstructure of the samples were further investigated by SEM and TEM (see Figure 2b-d). SEM images (Figure 2b and c) show that Pt-LDH-Foil samples have hierarchical porous structures, which consists of closely connected nanoplates with size of ca. 3 to 5 μm and the thickness ranging from 100 to 200 nm. Comparing the SEM image of Pt-LDH-Foil sample with that of LDH-Foil sample (not shown here), no obvious morphology change was found, indicating that the deposition of Pt NPs did not obviously change the morphology and microstructure of the LDH-Foil sample. SEM image (see Figure 2d) of cross-section of Pt-LDH-Foil sample indicates that the whole thickness of Pt-LDH-Foil sample is ca. 18 μm . Among them the thickness of LDH layer on Al foil surface is about 4 μm and the thickness of inner un-reacted Al layer within the sample is about 10 μm . The SEM observation indicates that only surface aluminium of Al foil was reacted to form Mg-Al layered

double hydroxide and the inner of Al foil still was metallic aluminium, which is consistent with the above XRD result.

TEM image (Figure 2e) of the Pt-LDH-Foil sample displays that many small Pt NPs with size of ca. 5-10 nm are uniformly deposited on the surface of the sample. These highly dispersed Pt NPs are beneficial for enhancing the rate of catalytic oxidation reaction of formaldehyde in air because they can provide more active centres for HCHO oxidation than the aggregated Pt NPs. EDX analyses were further performed for analysing the composition of Pt-LDH foil sample. Mg, Al, O and Pt elements were detected in the EDX spectrum (Figure 2f). Mg, Al and O are from Mg-Al LDHs and Pt is from the loading and deposition of Pt NPs, suggesting Pt NPs were successfully deposited on the surface of Mg-Al LDH nanoplates.

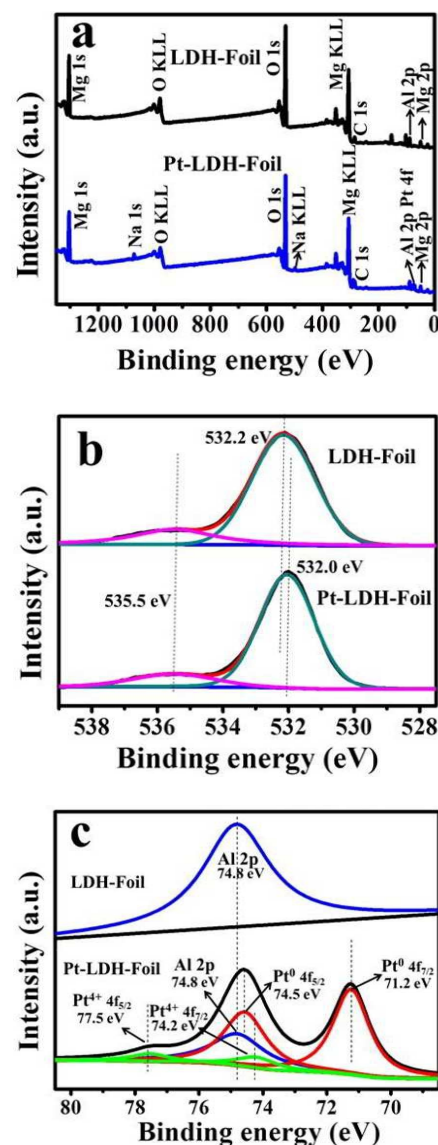


Figure 3. XPS survey spectra (a) of LDH-Foil and Pt-LDH-Foil samples, high-resolution XPS spectra for O 1s (b), Al 2p and Pt 4f (c) of LDH-Foil and Pt-LDH-Foil samples.

XPS analysis

The surface chemical composition and element chemical status of the prepared samples were investigated by X-ray photoelectron spectroscopy (XPS). The XPS survey spectra (Figure 3a) of LDH-Foil and Pt-LDH-Foil samples indicate the presence of Mg, Al, O and C elements for both samples, and their corresponding photoelectron peaks appear at binding energies of ca. 1303 (Mg 1s), 75 (Al 2p), 532 (O 1s), and 285 eV (C 1s). The peak of Na 1s is only observed in Pt-LDH-Foil sample because the Na species were introduced in the Pt loading process due to the use of NaBH₄ reactants. The C 1s XPS peak at the binding energy of 285 eV is due to the adventitious hydrocarbon, which originates from the XPS instrument itself.

High-resolution O 1s spectra of LDH-Foil and Pt-LDH-Foil (Figure 3b) show two peaks appearing at 535.5 and 532.0–532.2 eV, which can be assigned to adsorbed water (H₂O) and surface hydroxyl groups (Mg, Al-OH) in the Mg-Al double hydroxide, respectively.³⁹

⁴¹ High-resolution Al 2p spectra of LDH-Foil shows a peak at 74.8 eV, which can be assigned to Al 2p of Mg-Al layered double hydroxide.⁴² The high-resolution Pt 4f and Al 2p spectra of Pt-LDH-Foil show five peaks at 71.2, 74.5, 74.8, 74.2 and 77.5 eV, which correspond to Pt⁰ 4f_{7/2}, Pt⁰ 4f_{5/2}, Al 2p, Pt⁴⁺ 4f_{7/2} and Pt⁴⁺ 4f_{5/2}, respectively.^{18,39,43,44} The XPS results further demonstrate that Pt NPs were deposited on the surface of Mg-Al LDH.

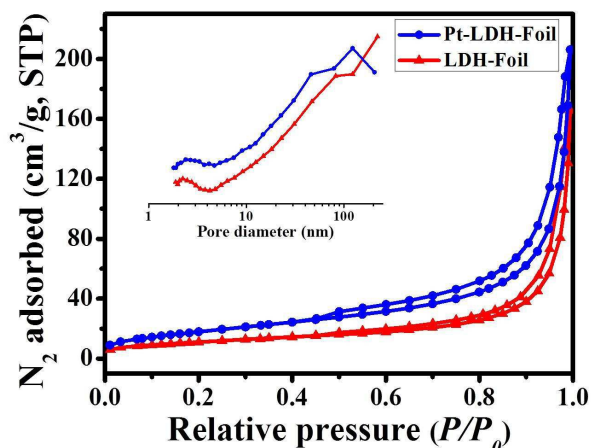


Figure 4. N₂ adsorption-desorption isotherms and the corresponding pore size distribution curves (inset) for the LDH-Foil and Pt-LDH-Foil samples.

Nitrogen adsorption

Nitrogen adsorption-desorption isotherms were measured to determine the specific surface areas and pore size distribution of the LDH-Foil and Pt-LDH-Foil samples (see Figure 4). Before nitrogen adsorption measurement, the LDHs and Pt-LDHs were scraped off from corresponding LDH-Foil and Pt-LDH-Foil samples and then measured. The isotherms corresponding to the above two samples are of type IV according to Brunauer-Deming-Deming-Teller (BDDT) classification and show high adsorption values at high relative pressure range of 0.9–1.0, indicating the existence of large mesopores and macropores.⁴⁵ The hysteresis loops are of type H3, indicating the presence of plate-like particles and slit-like pores.⁴⁶ The above results are in good agreement with the SEM images. The pore size distribution curves (inset) of two samples fitted from the adsorption branch of the nitrogen isotherm using the BJH (Barett-

Joyner-Halenda) method present a wide range of 10–100 nm. No great change in the shape of isotherms and pore size distribution curves between two samples is observed. This further suggests that the porous structure of LDH-Foil sample was well preserved after deposition of Pt NPs. These hierarchical mesopores and macropores can effectively act as gas-exchange channels for the gaseous formaldehyde and CO₂ products. The specific surface area of Pt-LDH-Foil (67 m²/g) sample is higher than that of LDH-Foil sample (41 m²/g). This is due to the generation of NaOH during the NaBH₄-reduction process, and the produced NaOH can etch the surface of the LDH-Foil sample, thus leading to the formation of numerous micropores and small mesopores, and the increase of specific surface area after Pt loading.

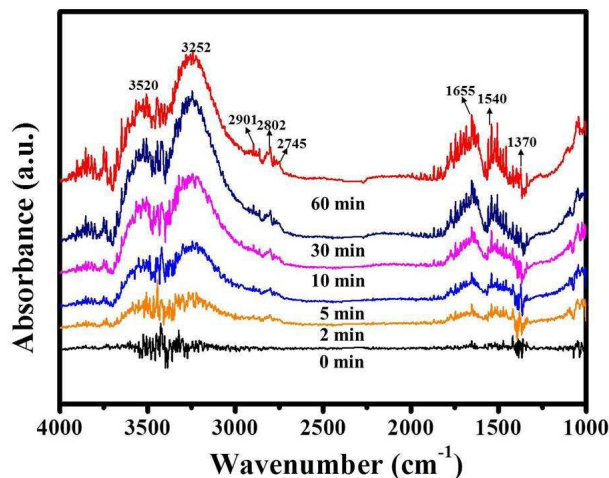


Figure 5. In situ DFTIR spectra of Pt-LDH-Foil catalyst as a function of time under a flow of HCHO/O₂ at room temperature.

In situ DFTIRS

In order to detect the intermediates in catalytic oxidation decomposition of formaldehyde and catalytic reaction mechanism, in situ DFTIR spectra were recorded. Figure 5 presents in situ DFTIR spectra of Pt-LDH-Foil catalyst upon exposure to HCHO/O₂ at room temperature at the different time. The sample was only exposed in HCHO/O₂ mixed gases for 2 min, the bands located at 1370 cm⁻¹ and 1540 cm⁻¹ are observed, which can be attributed to symmetric and asymmetric stretching of COO, respectively. This suggests that formate species are the intermediate products of HCHO oxidative decomposition and HCHO can be immediately oxidized into formate over the surface of Pt-LDH-Foil sample. There bands at 2745, 2802 and 2901 cm⁻¹ can be assigned to the stretching vibration of C-H, suggesting that HCHO molecules are adsorbed on the surface of the Pt-LDH-Foil samples. In addition, the bands at 1655, 3252 and 3520 cm⁻¹ are due to the produced water during the oxidation decomposition of formaldehyde.^{47,48}

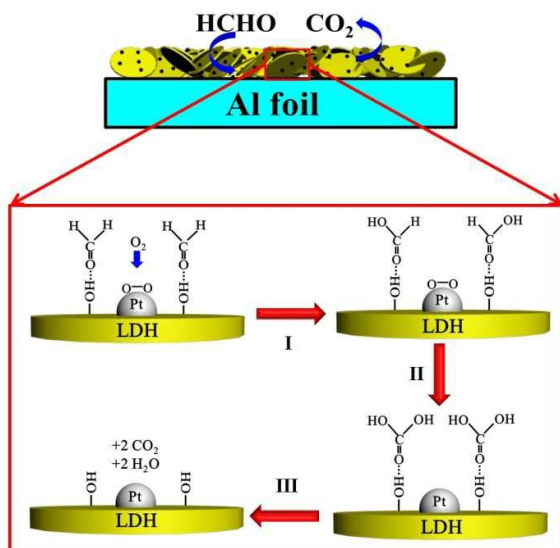


Figure 6. Suggested catalytic decomposition mechanism of formaldehyde at room temperature.

On the basis of the above results and discussion, the reaction mechanism for room temperature catalytic HCHO oxidation on the Pt-LDH-Foil is proposed and presented in Figure 6. Firstly, HCHO molecules are adsorbed on the surface hydroxyl via hydrogen bond and gaseous O₂ molecules are adsorbed and activated on the surface of Pt NPs.^{43,49,50} After that, adsorbed HCHO molecules are first oxidized into formate intermediates by activated oxygen atoms and the consumed O₂ molecules can be supplied from the air (step I). Then, the surface formate species are further oxidized into adsorbed carbonic acid (step II). The produced carbonic acid is very unstable and will rapidly decompose into CO₂ and H₂O, which will finally desorb from the sample surface, and the catalyst is regenerated (step III). Obviously, hydroxyl groups of Pt-LDH-Foil surface are beneficial to the above catalytic reaction because they can efficiently capture the gaseous HCHO molecules and intermediate products, thus resulting in the increase of oxidation reaction rate of HCHO. Meanwhile, hierarchical macro-/mesopores of Pt-Mg-Al LDH samples is also favourable to formaldehyde oxidation decomposition.^{23,51} The hierarchical porous structure not only allows most of the Pt NPs more exposed to gas reactants, but also reduces the diffusion resistance for the exchange of reactants (O₂ and HCHO) and products (CO₂ and H₂O), thus accelerating the reaction and decomposition rate of gaseous formaldehyde molecules. As a result, not surprising, the prepared flexible Pt-LDH-Foil sample exhibited a good room temperature catalytic HCHO oxidation activity.

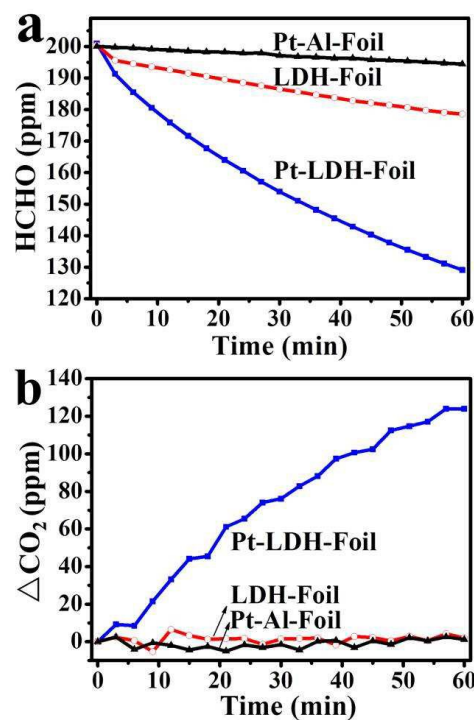


Figure 7. Changes in the decrease of formaldehyde concentration (a) and the increase of CO₂ concentration Δ CO₂ (the difference in CO₂ concentration between t time and initial time) (b) for Pt-Al-Foil, LDH-Foil and Pt-LDH-Foil samples used in the room temperature catalytic decomposition of formaldehyde.

Evaluation of catalytic activity

The catalytic activity of the LDH-Foil, Pt-Al-Foil and Pt-LDH-Foil samples toward HCHO catalytic decomposition at room temperature are shown in Figure 7. As can be seen in this figure, the concentration of HCHO only slightly decreases, and the concentration of CO₂ nearly keep almost unchanged during the whole HCHO catalytic oxidation for LDH-Foil and Pt-Al-Foil samples, indicating that these two samples have no catalytic activities toward HCHO oxidation. Contrarily, for Pt-LDH-Foil sample, not only the HCHO concentration greatly decrease, but also the CO₂ concentration increase simultaneously with increasing reaction time, suggesting that formaldehyde was completely decomposed into CO₂ and H₂O. Further observation from Figure 7 indicates that the increase of CO₂ concentration is slightly higher than the decrease of HCHO concentration. Not surprising, because some HCHO molecules were desorbed from the reactor surface with decreasing the HCHO concentration in the reactor. These desorbed HCHO molecules were further oxidized into CO₂, which result in the increase of CO₂ concentration.

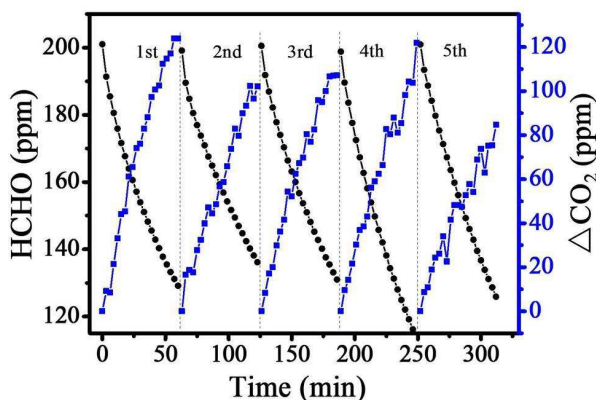


Figure 8. Changes in formaldehyde concentration and the produced CO_2 concentration as a function of reaction time for Pt-LDH-Foil sample in recycling tests.

The stability and repeatability of an indoor air purification catalyst is also important for its practical application. The stability and recyclability of the Pt-LDH-Foil sample were measured for catalytic decomposition of HCHO at room temperature and the related results are presented in Figure 8. The results indicated that the decrease rate of HCHO concentration and the increase rate of CO_2 concentration (see Figure 8) have no great change comparing with those observed in the first-cycle. The stability experiment suggests that the Pt-LDH-Foil sample has good repeatability and can maintain a good catalytic performance during the room temperature catalytic decomposition of formaldehyde.

4. Conclusion

Flexible and bendable Mg-Al LDHs grown on aluminum foil supported Pt catalyst was successfully prepared by a hydrothermal treatment of Al foil in the presence of $\text{Mg}(\text{NO}_3)_2$ and urea, followed by a NaBH_4 -reduction deposition of Pt NPs. The prepared Pt-LDH-Foil catalyst has hierarchically macro-/mesoporous structure and high specific surface area for the deposition of Pt NPs. The hierarchically porous structures are beneficial for reducing the diffusion resistance of gaseous reactants and products, thus enhancing the catalytic decomposition rate of HCHO molecules. In addition, abundant surface hydroxyl groups of Pt-LDH-Foil catalyst can act as adsorption centres of HCHO molecules, which is necessary in a typical gas-solid catalytic reaction. On the other hand, the flexible Pt-LDH-Foil catalyst exhibited good stability and repeatability. The above merits make this catalyst efficient in room temperature catalytic decomposition of formaldehyde and convenient in its practical application due to its light weight and easy preparation. Besides, considering the good flexibility and bendability of the Pt-LDH-Foil catalyst, this work will provide some new insight into the design and fabrication of efficient and practical catalyst for indoor HCHO purification.

Acknowledgements

This study was partially supported by the 973 program (2013CB632402), NSFC (21433007, 51320105001, 21573170,

51372190 and 51272199), Deanship of Scientific Research (DSR) of King Abdulaziz University (90-130-35-HiCi), the Fundamental Research Funds for the Central Universities (2015-III-034), Self-determined and Innovative Research Funds of SKLWUT (2015-ZD-1) and the Natural Science Foundation of Hubei Province of China (No. 2015CFA001)

References

- J. J. Collins, R. Ness, R. W. Tyl, N. Krivanek, N. A. Esmen and T. A. Hall, A review of adverse pregnancy outcomes and formaldehyde exposure in human and animal studies, *Regul. Toxicol. Pharm.*, 2001, **34**, 17-34.
- T. Salthammer, S. Mentese and R. Marutzky, Formaldehyde in the indoor environment, *Chem. Rev.*, 2010, **110**, 2536-2572.
- H. Nakamura, K. Kato, Y. Masuda and K. Kato, Activity of formaldehyde dehydrogenase on titanium dioxide films with different crystallinities, *Appl. Surf. Sci.*, 2015, **329**, 262-268.
- H. Q. Rong, Z. Y. Liu, Q. L. Wu, D. Pan and J. T. Zheng, Formaldehyde removal by Rayon-based activated carbon fibers modified by P-aminobenzoic acid, *Cellulose*, 2010, **17**, 205-214.
- Q. B. Wen, C. T. Li, Z. H. Cai, W. Zhang, H. L. Gao, L. J. Chen, G. M. Zeng, X. Shu and Y. P. Zhao, Study on activated carbon derived from sewage sludge for adsorption of gaseous formaldehyde, *Bioresour. Technol.*, 2011, **102**, 942-947.
- L. Z. Wang, Adsorption of formaldehyde (HCHO) molecule on the SiC sheet: A first-principles study, *Appl. Surf. Sci.*, 2012, **258**, 6688-6691.
- Z. H. Xu, J. G. Yu, G. Liu, B. Cheng, P. Zhou and X. Y. Li, Microemulsion-assisted synthesis of hierarchical porous $\text{Ni}(\text{OH})_2/\text{SiO}_2$ composites toward efficient removal of formaldehyde in air, *Dalton Trans.*, 2013, **42**, 10190-10197.
- F. Lin, G. Q. Zhu, Y. N. Shen, Z. Y. Zhang and B. Dong, Study on the modified montmorillonite for adsorbing formaldehyde, *Appl. Surf. Sci.*, 2015, **356**, 150-156.
- Z. H. Xu, J. G. Yu and W. Xiao, Microemulsion-assisted preparation of a mesoporous ferrihydrite/ SiO_2 composite for the efficient removal of formaldehyde from air, *Chem. Eur. J.*, 2013, **19**, 9592-9598.
- Z. H. Xu, J. G. Yu, J. X. Low and M. Jaroniec, Microemulsion-Assisted Synthesis of Mesoporous Aluminum Oxyhydroxide Nanoflakes for Efficient Removal of Gaseous Formaldehyde, *ACS Appl. Mater. Interfaces*, 2014, **6**, 2111-2117.
- R. X. Wang, R. X. Zhu and D. J. Zhang, Adsorption of formaldehyde molecule on the pristine and silicon-doped boron nitride nanotubes, *Chem. Phys. Lett.*, 2008, **467**, 131-135.
- J. J. Pei and J. S. S. Zhang, On the performance and mechanisms of formaldehyde removal by chemi-sorbents, *Chem. Eng. J.*, 2011, **167**, 59-66.
- J. G. Yu, X. Y. Li, Z. H. Xu and W. Xiao, NaOH-modified ceramic honeycomb with enhanced formaldehyde adsorption and removal performance, *Environ. Sci. Technol.*, 2013, **47**, 9928-9933.
- M. B. Chang and C. C. Lee, Destruction of Formaldehyde with Dielectric Barrier Discharge Plasmas, *Environ. Sci. Technol.*, 1995, **29**, 181-186.
- W. J. Liang, J. Li, J. X. Li, T. Zhu and Y. Q. Jin, Formaldehyde removal from gas streams by means of NaNO_2 dielectric barrier discharge plasma, *J. Hazard. Mater.*, 2010, **175**, 1090-1095.
- X. Fan, T. L. Zhu, Y. F. Sun and X. Yan, The roles of various plasma species in the plasma and plasma-catalytic removal of low-concentration formaldehyde in air, *J. Hazard. Mater.*, 2011, **196**, 380-385.
- Z. N. Han, V. W. Chang, X. P. Wang, T. T. Lim and L. Hildemann, Experimental study on visible-light induced photocatalytic oxidation

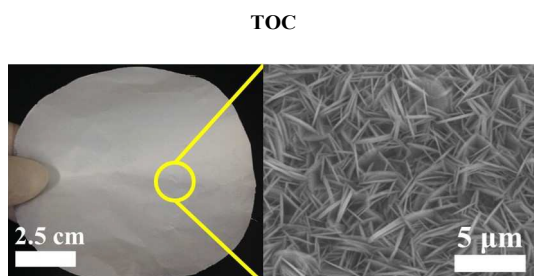
- of gaseous formaldehyde by polyester fiber supported photocatalysts, *Chem. Eng. J.*, 2013, **218**, 9-18.
18. P. F. Fu and P. Y. Zhang, Characterization of Pt-TiO₂ film used in three formaldehyde photocatalytic degradation systems: UV254 (nm), O₃+UV254 (nm) and UV254+185 (nm) via X-ray photoelectron spectroscopy, *Chin. J. Catal.*, 2014, **35**, 210-218.
 19. C. L. Wu, Facile one-step synthesis of N-doped ZnO micropolyhedrons for efficient photocatalytic degradation of formaldehyde under visible-light irradiation, *Appl. Surf. Sci.*, 2014, **319**, 237-243.
 20. H. B. Huang and D. Y. C. Leung, Complete Oxidation of Formaldehyde at Room Temperature Using TiO₂ Supported Metallic Pd Nanoparticles, *ACS Catal.*, 2011, **1**, 348-354.
 21. C. B. Zhang, F. D. Liu, Y. P. Zhai, H. Ariga, N. Yi, Y. C. Liu, K. Asakura, M. Flytzani-Stephanopoulos and H. He, Alkali-Metal-Promoted Pt/TiO₂ Opens a More Efficient Pathway to Formaldehyde Oxidation at Ambient Temperatures, *Angew. Chem., Int. Ed.*, 2012, **51**, 9628-9632.
 22. N. H. An, W. L. Zhang, X. L. Yuan, B. Pan, G. Liu, M. J. Jia, W. F. Yan and W. X. Zhang, Catalytic oxidation of formaldehyde over different silica supported platinum catalysts, *Chem. Eng. J.*, 2013, **215**, 1-6.
 23. L. H. Nie, A. Y. Meng, J. G. Yu and M. Jaroniec, Hierarchically Macro-Mesoporous Pt/γ-Al₂O₃ Composite Microspheres for Efficient Formaldehyde Oxidation at Room Temperature, *Sci. Rep.*, 2013, **3**, 3215.
 24. H. Y. Chen, Z. B. Rui and H. B. Ji, Monolith-Like TiO₂ Nanotube Array Supported Pt Catalyst for HCHO Removal under Mild Conditions, *Ind. Eng. Chem. Res.*, 2014, **53**, 7629-7636.
 25. L. H. Nie, J. G. Yu and J. W. Fu, Complete Decomposition of Formaldehyde at Room Temperature over a Platinum-Decorated Hierarchically Porous Electrospun Titania Nanofiber Mat, *ChemCatChem*, 2014, **6**, 1983-1989.
 26. L. H. Nie, P. Zhou, J. G. Yu and M. Jaroniec, Deactivation and regeneration of Pt/TiO₂ nanosheet-type catalysts with exposed {001} facets for room temperature oxidation of formaldehyde, *J. Mol. Catal. A: Chem.*, 2014, **390**, 7-13.
 27. C. B. Zhang, Y. B. Li, Y. F. Wang and H. He, Sodium-Promoted Pd/TiO₂ for Catalytic Oxidation of Formaldehyde at Ambient Temperature, *Environ. Sci. Technol.*, 2014, **48**, 5816-5822.
 28. Z. H. Xu, J. G. Yu and M. Jaroniec, Efficient catalytic removal of formaldehyde at room temperature using AlOOH nanoflakes with deposited Pt, *Appl. Catal. B*, 2015, **163**, 306-312.
 29. Q. L. Xu, W. Y. Lei, X. Y. Li, X. Y. Qi, J. G. Yu, G. Liu, J. L. Wang and P. Y. Zhang, Efficient Removal of Formaldehyde by Nanosized Gold on Well-Defined CeO₂ Nanorods at Room Temperature, *Environ. Sci. Technol.*, 2014, **48**, 9702-9708.
 30. J. Wang, P. Zhang, J. Li, C. Jiang, R. Yunus and J. Kim, Room-Temperature Oxidation of Formaldehyde by Layered Manganese Oxide: Effect of Water, *Environ. Sci. Technol.*, 2015, **49**, 12372-12379.
 31. J. H. Zhang, Y. B. Li, L. Wang, C. B. Zhang and H. He, Catalytic oxidation of formaldehyde over manganese oxides with different crystal structures, *Catal. Sci. Technol.*, 2015, **5**, 2305-2313.
 32. J. L. Wang, R. Yunus, J. G. Li, P. L. Li, P. Y. Zhang and J. Kim, In situ synthesis of manganese oxides on polyester fiber for formaldehyde decomposition at room temperature, *Appl. Surf. Sci.*, 2015, **357**, 787-794.
 33. H. B. Huang, P. Hu, H. L. Huang, J. D. Chen, X. G. Ye and D. Y. C. Leung, Highly dispersed and active supported Pt nanoparticles for gaseous formaldehyde oxidation: Influence of particle size, *Chem. Eng. J.*, 2014, **252**, 320-326.
 34. L. F. Qi, W. K. Ho, J. L. Wang, P. Y. Zhang and J. G. Yu, Enhanced catalytic activity of hierarchically macro-mesoporous Pt/TiO₂ toward room-temperature decomposition of formaldehyde, *Catal. Sci. Technol.*, 2015, **5**, 2366-2377.
 35. X. F. Zhu, B. Cheng, J. G. Yu and W. K. Ho, Halogen poisoning effect of Pt-TiO₂ for formaldehyde catalytic oxidation performance at room temperature, *Appl. Surf. Sci.*, 2016, **364**, 808-814.
 36. N. H. An, Q. S. Yu, G. Liu, S. Y. Li, M. J. Jia and W. X. Zhang, Complete oxidation of formaldehyde at ambient temperature over supported Pt/Fe₂O₃ catalysts prepared by colloid-deposition method, *J. Hazard. Mater.*, 2011, **186**, 1392-1397.
 37. C. Y. Ma, D. H. Wang, W. J. Xue, B. J. Dou, H. L. Wang and Z. P. Hao, Investigation of Formaldehyde Oxidation over Co₃O₄-CeO₂ and Au/Co₃O₄-CeO₂ Catalysts at Room Temperature: Effective Removal and Determination of Reaction Mechanism, *Environ. Sci. Technol.*, 2011, **45**, 3628-3634.
 38. S. He, Y. F. Zhao, M. Wei, D. G. Evans and X. Duan, Fabrication of Hierarchical Layered Double Hydroxide Framework on Aluminum Foam as a Structured Adsorbent for Water Treatment, *Ind. Eng. Chem. Res.*, 2012, **51**, 285-291.
 39. M. J. F., S. W. F., S. P. E. and B. K. D., *Handbook of X-ray Photoelectron Spectroscopy*, Perkin-Elmer Corporation, Eden Prairie, MN, 1992.
 40. B. Nunes, A. P. Serro, V. Oliveira, M. F. Montemor, E. Alves, B. Saramago and R. Colaco, Ageing effects on the wettability behavior of laser textured silicon, *Appl. Surf. Sci.*, 2011, **257**, 2604-2609.
 41. D. H. Kim, M. G. Jeong, H. O. Seo and Y. D. Kim, Oxidation behavior of P3HT layers on bare and TiO₂-covered ZnO ripple structures evaluated by photoelectron spectroscopy, *Phys. Chem. Chem. Phys.*, 2015, **17**, 599-604.
 42. K. H. Goh, T. T. Lim and Z. L. Dong, Enhanced Arsenic Removal by Hydrothermally Treated Nanocrystalline Mg/Al Layered Double Hydroxide with Nitrate Intercalation, *Environ. Sci. Technol.*, 2009, **43**, 2537-2543.
 43. H. Huang, D. Y. C. Leung and D. Ye, Effect of reduction treatment on structural properties of TiO₂ supported Pt nanoparticles and their catalytic activity for formaldehyde oxidation, *J. Mater. Chem.*, 2011, **21**, 9647.
 44. L. F. Qi, B. Cheng, J. G. Yu and W. K. Ho, High-surface area mesoporous Pt/TiO₂ hollow chains for efficient formaldehyde decomposition at ambient temperature, *J. Hazard. Mater.*, 2016, **301**, 522-530.
 45. F. Dong, R. Wang, X. Li and W. K. Ho, Hydrothermal fabrication of N-doped (BiO)₂CO₃: Structural and morphological influence on the visible light photocatalytic activity, *Applied Surface Science*, 2014, **319**, 256-264.
 46. K. S. W. Sing, D. H. Everett, R. A. W. Haul, L. Moscou, R. A. Pierotti, J. Rouquerol and T. Siemieniowska, Reporting physisorption data for gas/solid systems with special reference to the determination of surface area and porosity, *Pure Appl. Chem.*, 1982, **54**, 2201-2218.
 47. T. Kecskes, J. Rasko and J. Kiss, FTIR and mass spectrometric studies on the interaction of formaldehyde with TiO₂ supported Pt and Au catalysts, *Appl. Catal. A-Gen.*, 2004, **273**, 55-62.
 48. Z. X. Yan, Z. H. Xu, J. G. Yu and M. Jaroniec, Highly Active Mesoporous Ferrihydrite Supported Pt Catalyst for Formaldehyde Removal at Room Temperature, *Environ. Sci. Technol.*, 2015, **49**, 6637-6644.
 49. P. Zhou, X. F. Zhu, J. G. Yu and W. Xiao, Effects of Adsorbed F, OH, and Cl Ions on Formaldehyde Adsorption Performance and Mechanism of Anatase TiO₂ Nanosheets with Exposed {001} Facets, *ACS Appl. Mater. Interfaces*, 2013, **5**, 8165-8172.
 50. P. Zhou, J. G. Yu, L. H. Nie and M. Jaroniec, Dual-dehydrogenation-promoted catalytic oxidation of formaldehyde on alkali-treated Pt

ARTICLE

Journal Name

clusters at room temperature, *J. Mater. Chem. A*, 2015, **3**, 10432-10438.

51. L. F. Qi, B. Cheng, W. K. Ho, G. Liu and J. G. Yu, Hierarchical Pt/NiO Hollow Microspheres with Enhanced Catalytic Performance, *ChemNanoMat*, 2015, **1**, 58-67.



Flexible and bendable Mg-Al layered double hydroxide supported Pt catalysts fabricated and used in room-temperature catalytic decomposition of formaldehyde.